Received: 30 October 2019 | Revised: 12 November 2019 | Accepted: 13 November 2019

DOI: 10.1002/prp2.554

ORIGINAL ARTICLE

# LCAT protects against Lipoprotein-X formation in a murine model of drug-induced intrahepatic cholestasis

Marcelo J. A. Amar[1] | Lita A. Freeman[1] | Takafumi Nishida[1] | Maureen L. Sampson[1] | Milton Pryor[1] | Boris L. Vaisman[1] | Edward B. Neufeld[1] | Sotirios K. Karathanasis[1,2,3] | Alan T. Remaley[1]

[1]Lipoprotein Metabolism Section, Translational Vascular Medicine Branch, National Heart Lung and Blood Institute, National Institutes of Health, Bethesda, MD, USA

[2]Cardiovascular and Metabolic Disease Section, MedImmune, Gaithersburg, MD, USA

[3]NeoProgen, Baltimore, MD, USA

**Correspondence**
Marcelo J. A. Amar, National Institutes of Health, Building 10, Room 5D-03A, 10 Center Drive MSC 1666, Bethesda, MD 20892.
Email: ma90x@nih.gov

**Funding information**
National Heart, Lung, and Blood Institute; National Institutes of Health; MedImmune Inc

## Abstract

Familial lecithin:cholesterol acyltransferase (LCAT) deficiency (FLD) is a rare genetic disease characterized by low HDL-C levels, low plasma cholesterol esterification, and the formation of Lipoprotein-X (Lp-X), an abnormal cholesterol-rich lipoprotein particle. LCAT deficiency causes corneal opacities, normochromic normocytic anemia, and progressive renal disease due to Lp-X deposition in the glomeruli. Recombinant LCAT is being investigated as a potential therapy for this disorder. Several hepatic disorders, namely primary biliary cirrhosis, primary sclerosing cholangitis, cholestatic liver disease, and chronic alcoholism also develop Lp-X, which may contribute to the complications of these disorders. We aimed to test the hypothesis that an increase in plasma LCAT could prevent the formation of Lp-X in other diseases besides FLD. We generated a murine model of intrahepatic cholestasis in LCAT-deficient (KO), wild type (WT), and LCAT-transgenic (Tg) mice by gavaging mice with alpha-naphthylisothiocyanate (ANIT), a drug well known to induce intrahepatic cholestasis. Three days after the treatment, all mice developed hyperbilirubinemia and elevated liver function markers (ALT, AST, Alkaline Phosphatase). The presence of high levels of LCAT in the LCAT-Tg mice, however, prevented the formation of Lp-X and other plasma lipid abnormalities in WT and LCAT-KO mice. In addition, we demonstrated that multiple injections of recombinant human LCAT can prevent significant accumulation of Lp-X after ANIT treatment in WT mice. In summary, LCAT can protect against the formation of Lp-X in a murine model of cholestasis and thus recombinant LCAT could be a potential therapy to prevent the formation of Lp-X in other diseases besides FLD.

KEYWORDS

cholesterol acyltransferase, cholesterol acyltransferase deficiency, deficient mouse, Familial lecithin, intrahepatic cholestasis, LCAT transgenic mouse, lecithin, Lipoprotein-X

**Abbreviations:** ABCA1, ATP-binding cassette transporter A1; ACS, acute coronary syndrome; ApoA-I, apolipoprotein A-I; ApoC-II, apolipoprotein C-II; ApoC-III, apolipoprotein C-III; FFA, free fatty acids; HDL, high-density lipoprotein; KO, knockout; LDL, low-density lipoprotein; LPL, lipoprotein lipase; *Mdr2*, multidrug-resistant protein; PGP, P-glycoprotein; Tg, transgenic; TG, triglycerides; VLDL, very low-density lipoprotein.

This is an open access article under the terms of the Creative Commons Attribution-NonCommercial-NoDerivs License, which permits use and distribution in any medium, provided the original work is properly cited, the use is non-commercial and no modifications or adaptations are made.
© 2019 The Authors. *Pharmacology Research & Perspectives* published by John Wiley & Sons Ltd, British Pharmacological Society and American Society for Pharmacology and Experimental Therapeutics.

## 1 | INTRODUCTION

Lipoprotein-X (Lp-X) was first reported almost 50 years ago as an abnormal lipoprotein particle.[1] Lp-X is a multilamellar vesicle that primarily consist of free cholesterol and phospholipids with an aqueous core. Unlike normal lipoproteins, it is relatively devoid of core hydrophobic lipids and has a limited amount of exchangeable apolipoproteins that normally stabilize the structure of a lipoprotein.[2] Lp-X is heterogeneous in structure and can range in size from 30 to 100 nm and also has a relatively broad density range.[3] It is most readily identified by agarose gel electrophoresis, because it migrates toward the cathode, whereas normal lipoproteins migrate toward the anode.[4,5]

Lp-X has been reported in patients with both extrahepatic and intrahepatic obstructive type liver diseases, such as obstructive jaundice from gallstones,[6] primary biliary cirrhosis,[7] sclerosing cholangitis,[8] intrahepatic cholestasis of pregnancy,[9] and alcoholic hepatitis.[10] It can also occur in children with a genetic abnormality in the development of the liver, such as biliary atresia[11] and Allagile Syndrome.[12] It is also frequently seen in bone marrow transplant patients with cholestasis from graft-vs-host disease in which the majority of plasma cholesterol can become associated with Lp-X rather than LDL or HDL.[13]

The formation of Lp-X in these different types of liver disorders is not clearly understood but is thought to be a consequence of the retrograde movement of lipid micelles from bile, which are rich in phospholipids and free cholesterol, into the plasma. Bile salts stabilize biliary lipid micelles, but they are rapidly cleared from the plasma by the liver, causing the biliary lipid micelles to reorganize into Lp-X particles.[14] In fact, one can readily make Lp-X like particles by adding bile to plasma and dialyzing away the bile salts.[15]

The other condition in which Lp-X particles can form is Familial Lecithin:Cholesterol Acyltransferase (LCAT) Deficiency (FLD).[16] Lp-X particles accumulate in mesangial cells of the kidney where they induce inflammation.[17] It has been shown in mice that injection of Lp-X can cause proteinuria and is nephrotoxic.[18] Furthermore, recombinant LCAT can prevent Lp-X formation and renal disease in a mouse model of LCAT deficiency.[19] Because LCAT has a half-life of several days, a recombinant form of LCAT has been developed as a potential enzyme replacement therapy for FLD.[20-22] FLD patients, however, do not typically develop cholestasis so the mechanism for formation of Lp-X in this disorder is thought to be different than in cholestatic liver disease.

Now that there is a potential treatment for lowering Lp-X in FLD, it is of interest whether recombinant LCAT could also lower Lp-X in cholestatic liver disease. Lp-X in FLD and liver disease are morphologically similar based on electron microscopy, but a careful lipid and protein composition study comparing Lp-X from these different diseases has never been reported. The role of Lp-X in the pathogenesis of liver disease is also not known, but it has been demonstrated that Lp-X from cholestatic patients is readily taken up by macrophages[23] and hence could contribute to atherosclerosis. It also likely accounts for the severe xanthomas that some patients with cholestasis can develop, such as in Allagile Syndrome.[12] In at least two models of cholestasis in the dog, Lp-X has been linked to the pathogenesis of renal disease.[24,25] Patients with very high levels of Lp-X from liver disease are also sometimes acutely treated by plasmapheresis when they develop hyperviscosity syndrome, which can be life threatening.[26,27]

In this study, we used alpha-naphthylisothiocyanate (ANIT) to induce cholestasis[28] in LCAT-deficient (KO), control wild type (WT) and LCAT-transgenic (Tg) mice. Like in FLD, increasing plasma LCAT in cholestatic mice was shown to lower Lp-X formation from drug-induced cholestasis, whether by overexpressing an LCAT transgene or by injecting rhLCAT. Our results indicate that recombinant LCAT could have a wider therapeutic indication than just FLD.

## 2 | MATERIAL AND METHODS

### 2.1 | Reagents

α-Naphthylisothiocyanate (ANIT) was purchased from Sigma-Aldrich Co. (cat #18951-1) and diluted in corn oil. Recombinant human LCAT (rhLCAT) (MEDI6012) was provided by MedImmune, Gaithersburg, MD, USA and utilized as described in Figure 6.

### 2.2 | Mice and diets

Male C57Bl/6 (Jackson Laboratory), human LCAT-Tg,[29] and LCAT-KO[30] mice were fed a regular rodent chow diet (NIH-07 chow diet: 0.025% cholesterol, 4.5% fat; Ziegler Brothers, Inc). Mice were fasted overnight and treated with a single dose of ANIT by gavage (100 mg/kg in 100 μL). In some cases, LCAT (25 mg/kg BW) was injected, IP, two times per day on days 1 and 2 and once on day 3. Blood samples were collected from the periorbital sinus of the contralateral eye with a heparinized capillary tube (50 or 250 μL) at 0, 24, 48, 72, and 96 hours after gavage and placed into tubes with EDTA as an anticoagulant (final concentration, 4 mmol/L). Plasma was obtained after centrifugation for 10 min at 3000*g* at 4°C. Initially, experiments were terminated on day 4, but since not all mice survived to day 4, later experiments were terminated at day 3. All studies were based on 2 or more experiments with a minimal sample size of 3-5 mice per group. Repeated key experiments are showed as Supplemental Figures as indicated. All animal studies were approved by the NHLBI Animal Care and Use Committee (protocols # H-0050, H-0018).

### 2.3 | LCAT activity assay

Five microliters of plasma from mice were incubated with BODIPY-cholesterol proteoliposomes and separated by thin-layer chromatography. BODIPY-free cholesterol and BODIPY- cholesteryl ester were then quantitated on a Typhoon 9400 Variable Mode Imager

(GE Healthcare) set at 488 nm for excitation and 520 nm for emission, as described previously.[31]

### 2.4 | Analysis of plasma biomarkers, lipids, and lipoproteins

Lipids (total cholesterol, triglycerides and phospholipids), Alkaline Phosphatase, ALT, AST, and Bilirubin were measured enzymatically on a Roche Cobas-600. Plasma lipids were measured enzymatically (Wako Chemicals USA, Inc Richmond, VA) on a ChemWell-2910 analyzer (Awareness Technology, Inc, Palm City, FL).

### 2.5 | Lp-X and lipoprotein separation

Ten microliters EDTA-plasma or purified human lipoproteins (LDL, VLDL, and HDL) were loaded on Sebia Hydragel 15/30 lipoprotein(e) agarose gels (#4134; Sebia, Inc). Electrophoresis was performed for 1 hour at 100 V in barbital buffer (#B5934-12VL; MilliporeSigma) in a Titan Gel electrophoresis chamber (Helena Laboratories). Gels were either fixed and stained with Sudan Black to detect neutral lipids or incubated with Filipin Stain to detect free cholesterol exactly as described in reference.[5] Lp-X, which migrates toward the cathode in the opposite direction as normal lipoproteins, was quantified by densitometry of the cathode-migrating band in filipin-stained gels, and background in an equal-sized area of the gel 1 cm below the bottom of each band was subtracted using Alpha Imager software as described in Freeman et al, 2019.[5]

### 2.6 | Fast protein liquid chromatography

Plasma lipoproteins were fractionated by fast protein liquid chromatography (FPLC, Akta FPLC; GE Healthcare) on two Superose 6 columns in series.[32] Lp-X was detected in plasma by electrophoresis in Sebia Hydragel Lipoprotein (E) 15/30 gels, as described above.

### 2.7 | Statistical analysis

Unless otherwise indicated, all data are expressed as mean plus minus 1 SD. Mean values were compared by a two-tailed *T*-test and *P*-values <.05 were considered to be statistically significant.

## 3 | RESULTS

### 3.1 | ANIT study design

Three strains of mice with either high LCAT activity (LCAT-Tg; 1211 ± 120 U/mL/h), normal (WT, 15.5 ± 1.2 U/mL/h), or no LCAT activity (LCAT-KO; 1 ± 0.1 U/mL/h) with 83.1%, 78.4%, and 33.1% of cholesteryl esters, respectively, (baseline levels are shown in Table 1) were gavaged with ANIT at the start of the study. Plasma was collected and analyzed every 24 hour for 3-4 days.

**TABLE 1** Baseline lipid levels and LCAT activity

| | WT | LCAT-Tg | LCAT KO |
|---|---|---|---|
| Cholesterol (mg/dL) | 125.5 ± 37.5 | 235.8 ± 20.3* | 24.2 ± 4.7* |
| Free cholesterol (mg/dL) | 27.6 ± 6.2 | 39.8 ± 6.3* | 16.2 ± 3.3* |
| Cholesteryl ester (mg/dL) | 98.0 ± 33.0 | 196.0 ± 14.4* | 8.0 ± 1.6* |
| Triglycerides (mg/dL) | 136.3 ± 38.2 | 20.8 ± 9.7* | 220.7 ± 98.1* |
| Phospholipids (mg/dL) | 279.3 ± 51.5 | 299.6 ± 28.8 | 100.2 ± 16.2* |
| LCAT activity (U/mL/h) | 15.5 ± 1.2 | 1211 ± 120* | 1 ± 0.1* |

*Note:* Lipids (total cholesterol (TC), free cholesterol (FC), triglycerides, and phospholipids were measured following retro-orbital sinus blood collection (~75-100 μL; n = 7 mice/group) and plasma separation, enzymatically on a ChemWell-2910 analyzer. Cholesteryl esters (CE) were calculated utilizing the formula CE = TC − FC. LCAT activity was measured in 5 μL of plasma utilizing an endogenous assay, as described in Methods.

*$P < .05$ increase over baseline; n = average ± SD.

### 3.2 | ANIT differentially induces intrahepatic cholestasis in mouse models

Biomarker changes following ANIT treatment (Figure 1 and Figure S1) were similar to previously published reports[28] and represents two separate studies. At baseline, all three mouse strains of mice had similar levels of bilirubin, ALT, AST, and alkaline phosphatase Figure 1 and Figure S1A-F). By Day 2 after the ANIT gavage, there was a marked increase in total bilirubin in all three lines of mice (Figure 1A and B and Figure S1A and B) and plasma was visibly icteric. Both total and direct bilirubin, however, were higher in LCAT-KO mice compared to WT or LCAT-Tg mice at Day 2, and while these values plateaued by Day 4 for WT and LCAT-Tg mice they continued to increase sharply for LCAT-KO mice through the remainder of the study. The vast majority of the increase in bilirubin was direct or conjugated bilirubin, consistent with the known mechanism of ANIT in causing intrahepatic cholestasis.[33] Similarly, ALT and AST, markers of hepatic damage, also markedly increased after the ANIT treatment (Figure 1D and E and Figure S1D and E). In WT and LCAT-Tg mice, these markers peaked at day 2 and then started to return to baseline. In contrast, ALT and AST continued to increase by day 4 in LCAT-KO mice. Alkaline phosphatase, a marker of extrahepatic obstruction, was relatively flat the first few days, but then showed an increase, most pronounced for LCAT-KO mice, on day 4 (Figure 1F and Figure S1F). Overall, these results are consistent with the known effect of ANIT in causing intrahepatic cholestasis

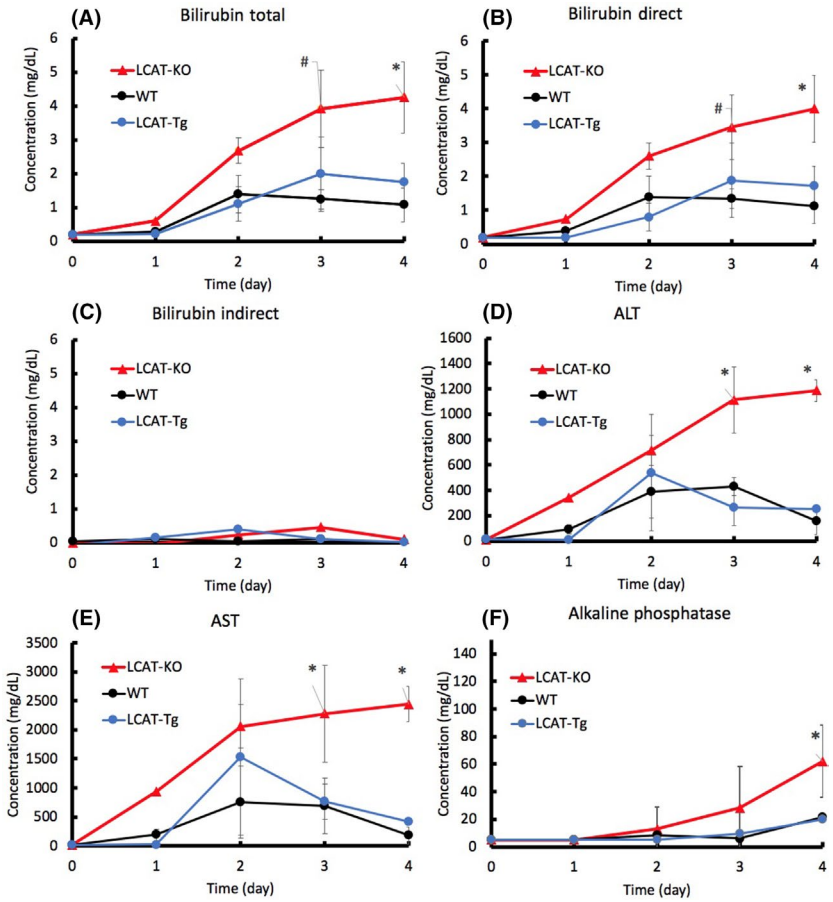


**FIGURE 1** Changes in hepatic function following treatment with ANIT. Mice (WT, LCAT-Tg, and LCAT-KO, males, n = 5 per group) were fasted for 4-6 hours and then bled by retro-orbital sinus blood collection (~75-100 μL). Mice were bled before, 1, 2, 3, and 4 days after ANIT gavage via the retro-orbital sinus. Hepatic function markers, Total Bilirubin (A), Direct Bilirubin (B), Indirect Bilirubin (C), ALT (D), AST (E), and alkaline phosphatase (F.) were measured as described in the Methods section. *$P$<.05 compared to WT and LCAT-Tg mice, #$P$<.05 compared to LCAT-Tg mice

and based on these biomarkers LCAT-KO mice appeared to be more sensitive to the ANIT treatment.

### 3.3 | LCAT level alters response to changes in lipoprotein levels from ANIT-induced cholestasis

We next examined the impact of ANIT treatment on total plasma lipids in the three strains of mice expressing different levels of LCAT (Figure 2 and Figure S2). Table 1 illustrate the baseline values of the three groups of mice utilized in these experiments. Consistent with what is observed in FLD patients, LCAT-KO mice at baseline had lower TC than WT mice and it was mostly in the form of free (unesterified) cholesterol (Figure 2A and B, Figure S2A and B). In LCAT-KO mice, 33% of cholesterol was esterified at baseline and presumably represents ACAT-derived cholesteryl esters. ACAT is a hepatic enzyme and is the other source of plasma cholesteryl esters in lipoproteins secreted by the liver; it has been previously observed that cholesteryl esters derived from ACAT can increase in LCAT-KO mice when placed on a high-fat diet.[34]

TG levels were higher in LCAT-KO than in WT mice, again recapitulating the lipid phenotype of severe FLD patients and possibly compensating for the lack of plasma-derived CE (Figure 2C and Figure S2C). PL levels in plasma of LCAT-KO mice at baseline were almost 3X lower than in WT (Figure 2D and Figure S2D). Conversely, LCAT-Tg mice at baseline had lower plasma TG and slightly higher percentage of CE levels (83% vs 78% in WT), and markedly decreased CE compared to WT mice. PL levels in LCAT-Tg plasma were not significantly different than WT.

LCAT levels significantly altered the response to ANIT-induced cholestasis. By day 3, there was a 10-15-fold increase in plasma TC in the LCAT-KO mice, whereas in the WT and LCAT-Tg mice, TC increased to a much lesser degree (Figure 2A). In the first 2 days after ANIT treatment, free cholesterol showed the greatest increase in the LCAT-KO mice, whereas this increase was blunted in the LCAT-Tg mice, and WT mice showed an intermediate increase (Figure 2B). By day 3, all of the mice had similar levels of free cholesterol. Cholesteryl esters also increased in all three lines of mice, but the LCAT-KO mice showed the greatest increase when compared to baseline values (Figure 2E). Plasma TG, in contrast, decreased precipitously after ANIT treatment in the WT and LCAT-KO mice but increased by about 6-fold on day 3 in LCAT-Tg mice. Plasma phospholipids increased sharply in LCAT-KO mice throughout the time course (Figure 2D). WT mice PL's also increased markedly after Day 1, but LCAT-Tg PL's showed only a modest increase late in the time course, between Days 2 and 3.

### 3.4 | LCAT overexpression protects against the formation of Lp-X

To determine the plasma propensity of Lp-X formation, we plotted the ratio of surface lipids (free cholesterol and phospholipids)

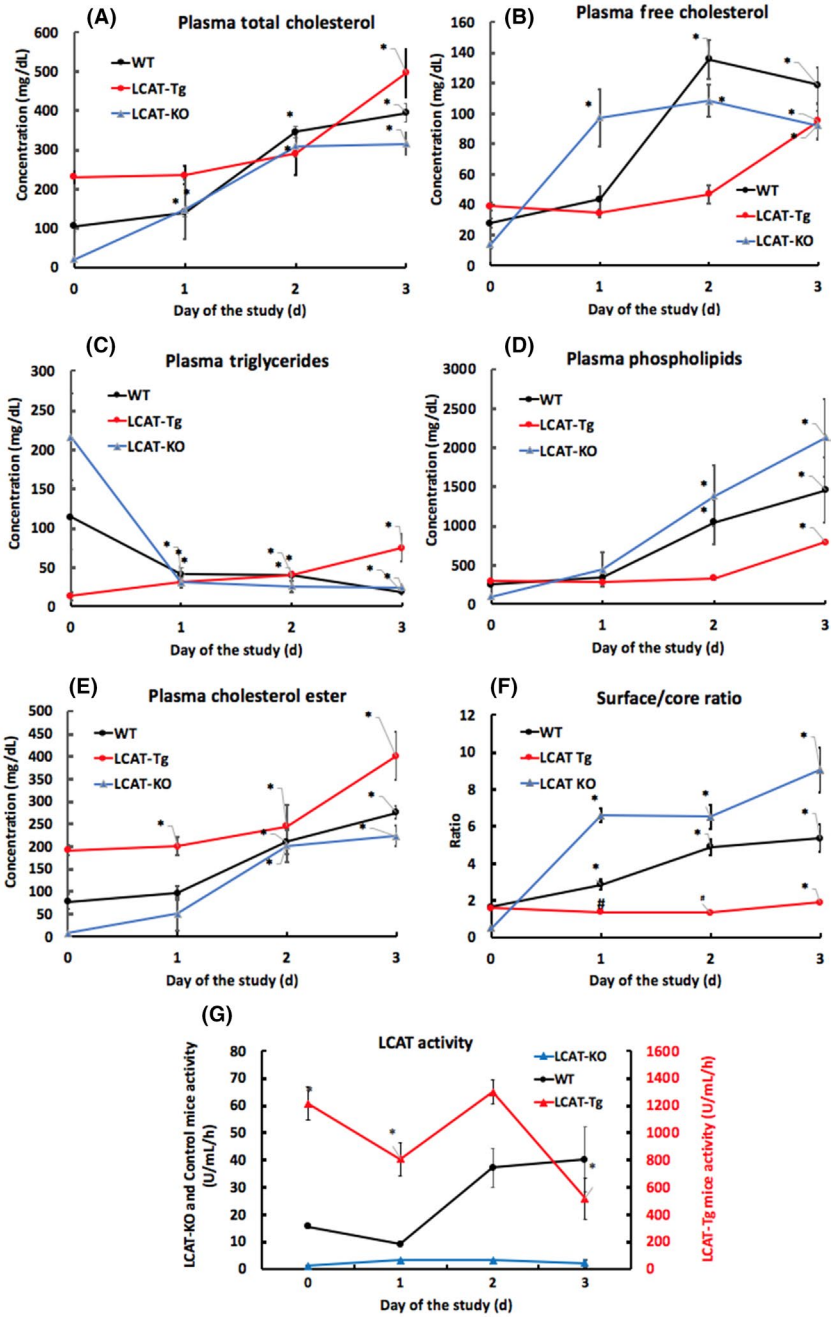


**FIGURE 2** Change in plasma lipid and lipoproteins following ANIT treatment. Mice (WT, LCAT-Tg, and LCAT-KO, males, n = 4 per group) were fasted for 4-6 hours and then bled by retro-orbital sinus blood collection (~75-100 μL). Mice were bled before, 1, 2, and 3 days after ANIT gavage via the retro-orbital sinus, until peak levels of Lp-X were present. Total Cholesterol (A), Free Cholesterol (B), Triglycerides (C), Phospholipids (D), Cholesteryl Ester (E) were measured as described in the Methods section. (F) surface/core lipid ratio, was calculated following the formula (FC + PL)/(CE + TG). (G) LCAT activity, was measured using endogenous substrate and calculated as described in the Methods section; red line represents the LCAT-Tg activity (red legend, right, red *x*-axis) while blue and black lines represent LCAT-KO and control mice, respectively (black legend, left *x*-axis). *$P$<.05 increase over baseline, #$P$<.05 decrease over baseline

to hydrophobic core lipids (TG and cholesteryl esters, Figure 2F). By day 1, this index markedly increased in the LCAT-KO mice and continued to increase over the 3 days. In contrast, this index remained relatively flat in LCAT-Tg mice. For WT mice, this index also increased after the ANIT treatment but remained below that observed for the LCAT-KO mice. When endogenous LCAT activity was measured (Figure 2G), we observed no significant decrease in activity, in fact, LCAT activity increased on day 2 and 3 in control mice, while in LCAT-Tg mice a transitory reduction was observed only on days 2 and 4, which could be related to changes in cholesterol availability for esterification during the study. These data suggest that LCAT overexpression may protect against the formation of Lp-X.

We next analyzed plasma lipoproteins by agarose gel electrophoresis followed by staining with Sudan Black, which stains neutral lipids (Figure 3, top), or Filipin, which stains free cholesterol and is more sensitive than Sudan Black in visualizing backwards-running Lp-X[5] (Figure 3, bottom). At baseline, several bands migrating toward the anode with mobilities in and around the apoB-containing-lipoproteins (apoB-Lp's) region (LDL and VLDL) could be seen with Sudan staining in LCAT-KO and WT mice (Figure 3, Sudan, Baseline). HDL could also be observed at baseline by Sudan staining in WT and LCAT-Tg mice, with the HDL band more prominent in the LCAT-Tg mice, as would be expected (Figure 3, Sudan, Baseline). In filipin-stained gels of mouse plasma at baseline, only a faint band corresponding to HDL could be seen

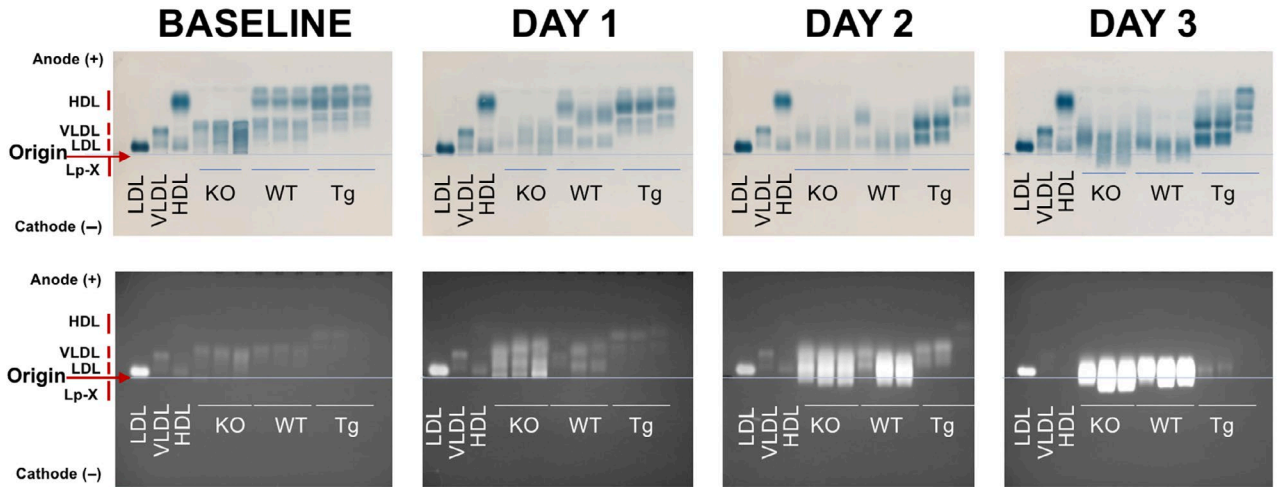


**FIGURE 3** Plasma lipoproteins by agarose gel electrophoresis. Plasma was obtained from mice (WT, n = 3, LCAT-Tg, n = 3and LCAT-KO, n = 3, males) either before (Baseline) or 1, 2, or 3 days after ANIT treatment (a single gavage of 100 mg/kg). 10 μL of plasma were loaded onto duplicate agarose gels followed by electrophoresis for 1 hour at 100 V. Gels were stained with Sudan Black (upper panels) or Filipin (lower panels) as described in Methods section. 10 μL of purified human LDL, VLDL, and HDL were included as standards loaded on the left side of each gel. Lp-X can be seen as backwards-running (ie cathode-migrating) fluorescent material by Filipin staining. The origin (point of application) is marked by a red arrow at the left of the gels and by a thin blue line running across the center of the gels. Vertical red lines to the left of the gels mark the regions where HDL, VLDL, LDL, and Lp-X migrate. HDL, LDL, and VLDL migrate towards the anode (+) and Lp-X migrates toward the cathode (–)

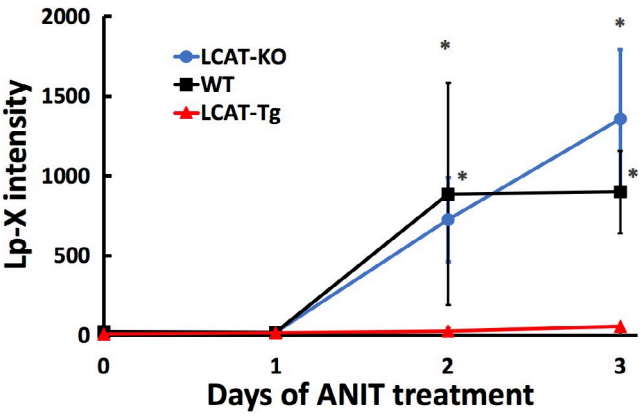


**FIGURE 4** Densitometric quantification of Lp-X in Filipin stained gels. The fluorescent cathode-migrating Lp-X signal for samples on each gel were normalized to the fluorescent purified LDL signal on each gel to ensure accurate comparisons between gels. Average Lp-X intensities (normalized to LDL) for each mouse line plus minus 1 SD are shown as a function of days after the ANIT treatment. WT; n = 3, LCAT-KO; n = 3 and LCAT-Tg; n = 3

in the LCAT-Tg mouse samples, whereas in the LCAT-KO and WT mice only faint bands in the region corresponding to VLDL and LDL could be observed (Figure 3, Filipin, Baseline). No cathodal migrating bands below the origin corresponding to Lp-X could be seen in any of the mouse lines at baseline.

On day 2 after ANIT treatment, cathodal migrating bands on filipin-stained gels corresponding to Lp-X could be observed in LCAT-KO and WT mice but not in LCAT-Tg mice and the intensity of the Lp-X band continued to increase up to day 3. The banding pattern observed after Filipin and Sudan Black staining was variable between mice on days 1 and 2 after ANIT treatment, but by day 3, there was a consistent and clear increase in the free cholesterol staining of anodal migrating bands corresponding to FC-enriched apoB-Lp's in LCAT-KO and WT mice but not in LCAT-Tg mice. This pattern persisted through day 3.

In Figure 4, we quantified the Lp-X bands after Filipin staining by densitometry, which clearly shows that Lp-X first appears 2 days after ANIT treatment in LCAT-KO and WT mice and increases in LCAT-KO mice on day 3. In contrast, no bands corresponding to Lp-X could be observed on any day after ANIT treatment in LCAT-Tg mice. The combined data demonstrate that increased LCAT expression in the LCAT-Tg mice clearly protected against the accumulation of Lp-X in plasma in this mouse model of drug-induced cholestasis.

### 3.5 | ANIT induces hepatic Lp-X formation

In Figure 5, we examined the liver tissue of mice by electron microscopy. Transmission electron microscopy (TEM) revealed that the overall architecture of the WT, LCAT-KO, and LCAT-Tg mouse livers were similar after ANIT treatment. The livers in all three strains of mice showed similar evidence for intrahepatic cholestasis from the ANIT treatment, consistent with what has been previously described.[35] We also looked for the appearance of Lp-X in liver compartments and whether this differed in the different mouse strains. Consistent with plasma we observed Lp-X in WT and LCAT-KO, but not LCAT-Tg, livers by TEM (Figure 5). As seen in Figure 5, Lp-X appears to have been taken up by Kupffer cells in WT and LCAT-KO liver. Additionally, we observed Lp-X in the sinusoids of LCAT-KO

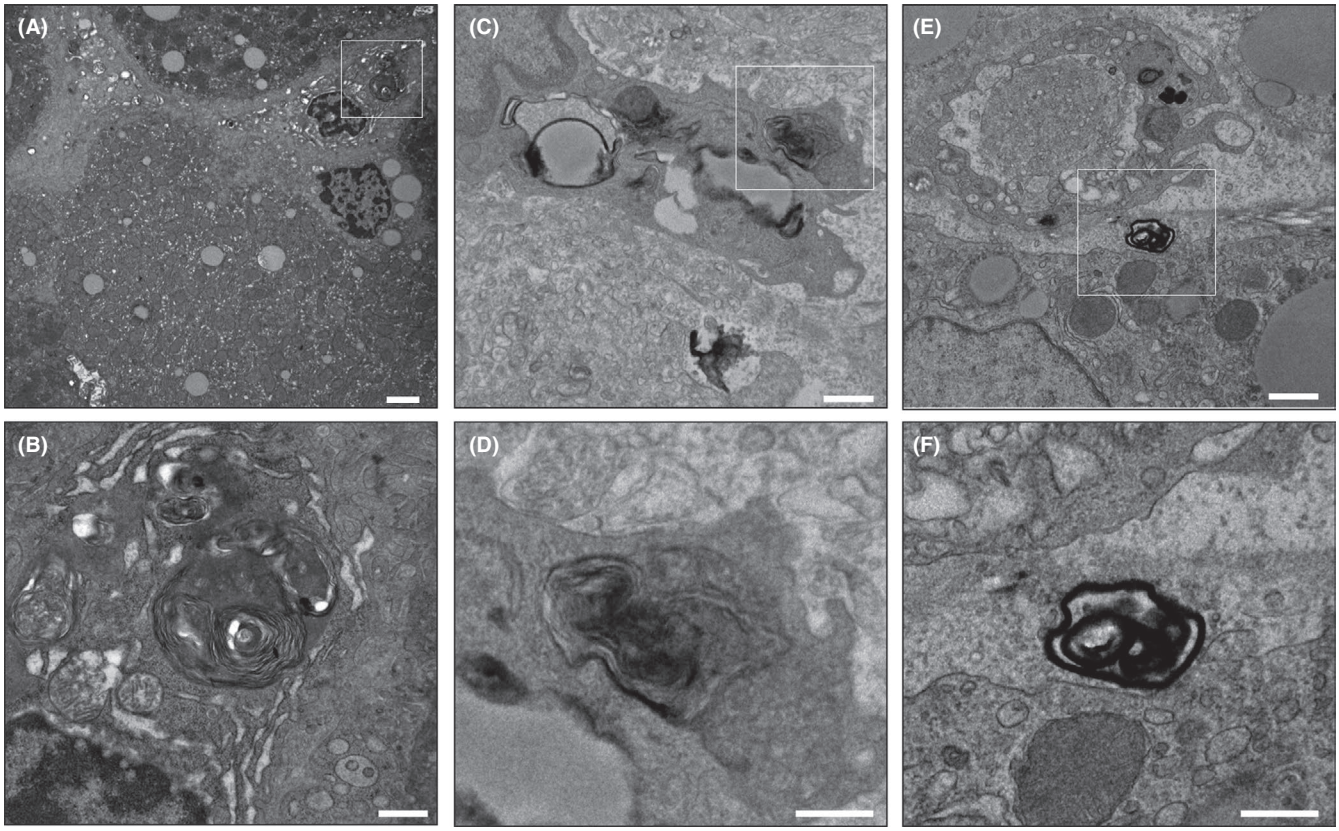


**FIGURE 5** Lp-X in WT and LCAT-KO mouse liver. Transmission electron microscopy reveals the appearance of multilamellar Lp-X in WT and LCAT-KO mouse liver compartments. Lp-X is taken up by Kupffer cells in WT (A, n = 40 slices) and LCAT-KO (C, n = 12 slices) mouse liver and is seen in hepatic sinusoids of LCAT-KO mice (E). Regions denoted by *white* boxes in (A), (C), and (E) are shown at higher magnification in (B), (D), and (F), respectively. Scale bars: (A): 2 μm; (B) 600 nm; (C): 800 nm; (D): 400 nm; (E): 1 μm; (F): 500 nm

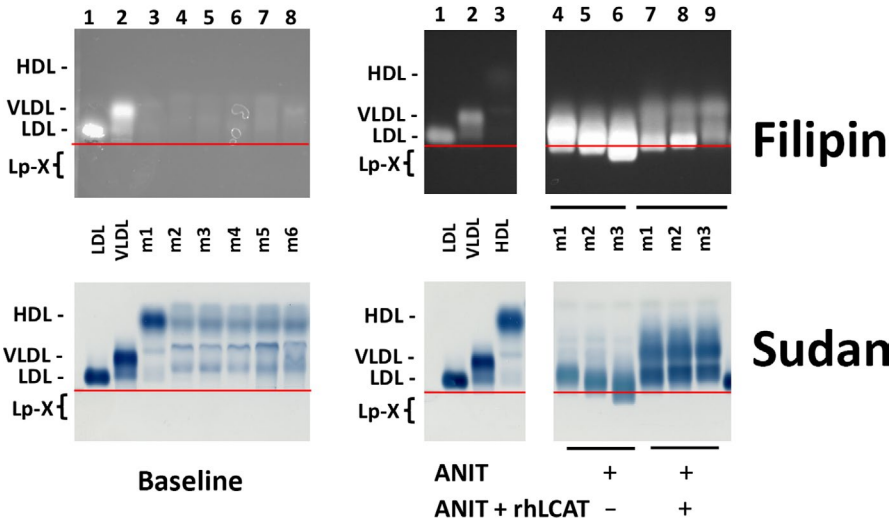


**FIGURE 6** In vivo treatment with rhLCAT reduces Lp-X in ANIT-induced cholestasis. WT mouse plasma electrophoresis at baseline (A), on day 3 after ANIT gavage and on day 3 after ANIT gavage with multiple in vivo injections of rhLCAT (B). Plasma of six WT mice (n = 6) is shown in (A). Following electrophoresis gels were staining with Filipin (top panels) or Sudan Black (bottom panels) as described in Figure 3. (A) lanes 1, 2 reflect the migration of purified human LDL and VLDL, respectively; lanes 3-8, WT mouse plasma of distinctive mice. (B) lanes 1-3 reflect the migration of purified human LDL, VLDL, and HDL respectively, lanes 4-6 reflect plasma from three individual WT mice plasma on day 3 after ANIT gavage; lanes 7-9 show the remodeling effect produced by treatment with rhLCAT, in vivo, on mouse plasma, on day 3 after ANIT gavage. Lp-X is visible by Filipin and, Sudan staining (mouse m3), in lanes 4-6 below the red (origin, point of application) line. LDL, VLDL, and HDL migrate toward the anode (+, top) and Lp-X migrates toward the cathode (–, bottom)

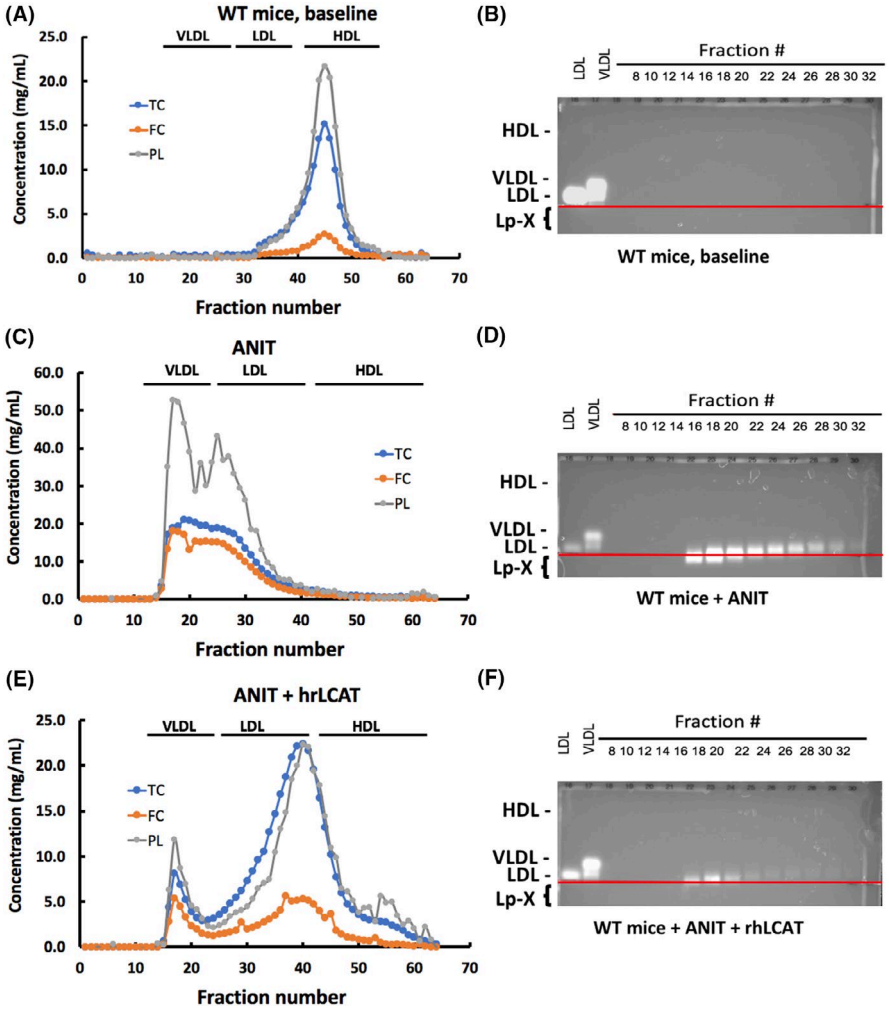


**FIGURE 7** Recombinant human LCAT injection reduces Lp-X in cholestatic murine plasma. FPLC analysis of WT mouse plasma at baseline (A and B), on day 3 after ANIT gavage (C and D) and on day 3 after ANIT gavage with multiple injections of rhLCAT in vivo (E and F). One hundred and fifty microliters of mouse plasma were separated through two Superose 6 columns in series producing 60 (0.5 mL each) fractions. Each fraction was analyzed for its cholesterol (total [TC] or unesterified [FC]) and phospholipid [PL] content as described in Methods section. LDL, VLDL, and HDL migrate toward the anode (+, top) and Lp-X migrates toward the cathode (–, bottom; B, D, and F). Typically, VLDL elutes in fractions 8-22, LDL elutes in fractions 23-32 and HDL elutes in fractions 35-60 (A, C, and E). (A, C, E) illustrates the TC, FC, and PL profile of a WT mouse (A), WT mouse plasma on day 3 after ANIT gavage (C) and WT mouse plasma on day 3 after ANIT gavage followed by multiple in vivo injections of rhLCAT (E). (B, D, F) illustrates the corresponding migration of fractions 8-32 (VLDL and LDL) on an agarose gel stained with Filipin as described in Figure 3. Lp-X is visible in fractions 15-35 on C and below the red (origin, point of application) line in D

cells. The Lp-X observed in ANIT-treated WT and LCAT-KO liver was similar in size and appearance to that previously observed in the liver and kidney of another cholestatic mouse model, the SREBP1a-Tg x LCAT-KO mouse. The SREBP1a-Tg x LCAT-KO mouse forms abundant amounts of Lp-X in the plasma and develops lipid droplets in hepatocytes with the appearance of multilamellar Lp-X particles in liver sinusoids and bile canaliculi. In the kidney, Lp-X is found in glomerular endothelial cells, podocytes, the glomerular basement membrane, the mesangium with presence of proteinuria (Vaisman et al, 2019 and Figure S4A [liver], B [liver, magnification], C [kidney], D [kidney, magnification]). Most notably, we could not find any intracellular or extracellular Lp-X in LCAT-Tg mouse liver unlike in WT or LCAT-KO mice.

### 3.6 | In vivo treatment with rhLCAT reduces Lp-X accumulation in plasma

Finally, to test the feasibility of whether LCAT can be used as a potential therapy for reducing Lp-X in cholestasis, we injected rhLCAT into WT mice treated with ANIT (Figures 6 and 7). Based on observations from previous clinical trials of rhLCAT,[21,22] we hypothesized that the increased esterification of cholesterol by the infused rhLCAT would remodel Lp-X into normal lipoproteins, as we observed in the LCAT-Tg mice experiments. Figure 6A shows the baseline lipoproteins of WT mice (m1 to m6) by agarose gels stained with Filipin (Figure 6A, top) or Sudan black (Figure 6A, bottom), prior to ANIT treatment. Because of the low FC content in these mice, only a faint signal of LDL and

VLDL are observed on the Filipin-stained gel, but all of the lipoproteins (LDL, VLDL, HDL) are clearly observed on the Sudan stained gels. Figure 6B illustrates the changes that occurred on day 3 after ANIT gavage in WT mice that did not (lanes 4-6) or did (lanes 7-9) receive rhLCAT treatment. In B, lanes 4-6, Lp-X can be seen migrating below the origin (highlighted in red). In mice injected with rhLCAT, we observed a marked reduction of any Lp-X band migrating below the origin for both the filipin and Sudan black stained gels (lanes 7-9). In the Sudan-stained gel after ANIT treatment (Figure 6B, bottom), the remodeling effects of rhLCAT can be seen in lanes 7-9 by the changes in the intensity of LDL and HDL bands, as previously reported.[5,18,20] This result suggests the redistribution of the newly esterified cholesterol from Lp-X lipids into these lipoproteins. Besides the decrease in Lp-X, another notable change in response to the rhLCAT treatment was an overall decrease in Filipin staining for all of the other lipoproteins, which we have also previously observed[5,18,20] and is consistent with the known ability of LCAT to esterify cholesterol.

The changes in lipids and lipoproteins after in vivo rhLCAT treatment were further examined in Figure 7 and Figure S3, which shows the distribution of plasma lipids after separation by FPLC. Figure 7A, C and E illustrate the TC, FC and PL profile of a WT mouse (Figure 7A), WT mouse plasma on day 3 after ANIT gavage (Figure 7C) and WT mouse plasma on day 3 after ANIT gavage followed by multiple injections of rhLCAT (Figure 7E), respectively. As before, ANIT dramatically modifies the lipoprotein distribution of WT mice by shifting of lipids from HDL (Figure 7A) to the VLDL/LDL region (Figure 7C). Figure 7D shows the presence of Lp-X in fractions 16-22 of the FPLC but increases of FC and PL were also observed in other fractions, indicating that besides causing Lp-X formation that the ANIT treatment also alters the lipid composition of normal lipoproteins. The remodeling led by the action of rhLCAT is illustrated in Figure 7E and F and shows major decrease in lipoprotein particles in the LDL and VLDL size ranges. In addition, Figure 7F demonstrates the near disappearance of the cathodic migrating Lp-X particles and a significant decrease of free cholesterol on other lipoproteins. Similar but lesser changes were found in lipoproteins and Lp-X levels in a separate independent study that used lower doses of rhLCAT for the treatment (Figure S3).

## 4 | DISCUSSION

In this study, we demonstrated that LCAT can prevent the formation of Lp-X during cholestasis, which is the most common cause of Lp-X formation.[36] In addition, we show feasibility from in vivo studies in mouse plasma that rhLCAT treatment, which has been shown to increase HDL-C levels and improve renal function in an LCAT-deficient patient,[21] could potentially be applicable to also lower Lp-X in cholestasis.

To acutely induce Lp-X formation, we used a previously established model of chemically induced intrahepatic cholestasis by treating mice with ANIT.[28] ANIT causes acute liver toxicity characterized by biliary epithelial injury, edema, neutrophilic infiltrate and other pathologic changes[37] similar to many other known drugs that can cause cholestasis.[38] The acute injury from ANIT, in the first 24-48 hours, leads to cessation of bile flow followed by increased levels of bile acids in plasma, significantly increasing the levels of phospholipids and unesterified cholesterol.[39] In addition, it causes elevation of various markers of liver damage (bilirubin, alkaline phosphatase, AST), and causes a marked increase in plasma levels of Lp-X.[28] Peak hepatic damage based on biomarkers occurs by 36-48 hours, and thereafter it starts to abate, with liver function tests typically returning to baseline ~96 hour after the initial ANIT treatment[39] similar to what we observed in our study.

As previously discussed, Lp-X is thought to form from the reflux of bile, which is rich in phospholipids and free cholesterol, into the plasma compartment.[15] Elferink et al demonstrated that the mouse *Mdr2* gene (homologous to the human *ABCB4* gene) is essential for Lp-X formation and its activity closely correlates with plasma Lp-X levels.[40] Mdr2 translocates phosphatidylcholine from the inner to the outer leaflet of the cell membrane, making it available for secretion into the liver bile canalicular lumen. Crawford and others[41] have concluded that adherent lipid vesicles are formed on the outer leaflet of the canalicular membrane and Lp-X is formed at these sites where Mdr2 is present. In addition, Arias et al[42] demonstrated the role of liver LKB1 trafficking of ABCB11 with the formation of Lp-X, but absence of ABCB11 can protect Mdr2 KO mice from cholestatic liver and bile duct injury.[43] Felker et al suggested that Lp-X formation takes place in an extracellular compartment, probably within the biliary canaliculi.[35] Once formed, Lp-X particles are believed to be transported by transcytosis to the sinusoidal space and then released into the plasma. In summary, LCAT can reduce the formation of Lp-X in a mouse model of cholestasis, which extends the possible indications for rhLCAT therapy.

Although liver damage was evident in all three mouse strains after ANIT administration, mice expressing LCAT (WT and LCAT-Tg mice) had substantially lower levels of ALT, AST, alkaline phosphatase, and conjugated bilirubin compared to mice lacking LCAT. The reason for this finding is unclear. It does not appear, however, to be correlated with the presence or absence of Lp-X, since WT mice had nearly as much Lp-X in plasma as LCAT-KO mice. One feature that distinguishes WT and LCAT-Tg mice from LCAT-KO mice is that WT and LCAT-Tg mice have HDL, whereas LCAT-KO mice, as we have shown in this study, have markedly reduced levels of HDL. Additional studies will be needed to address this hypothesis, but given the known anti-inflammatory properties and other beneficial properties of HDL[44,45] in a wide variety of diseases,[46] it may be that the absence of HDL in LCAT-KO mice made them more susceptible to hepatic damage from the ANIT treatment.

A major finding from this study is that LCAT can prevent the formation of Lp-X from cholestasis. We have previously shown that rhLCAT can promote both in vitro and in vivo dissolution of Lp-X formed due to LCAT deficiency.[5,19,20] In the case of Lp-X formed in LCAT deficiency, it has been shown that esterification of cholesterol by adding exogenous LCAT causes the Lp-X particles to spontaneously remodel and when Lp-X is treated with LCAT in the presence of apoA-I, HDL-like particles can be formed.[20] This suggests that the stability of Lp-X is largely due to the physiochemical properties of its lipid components, free cholesterol and phospholipid. When cholesterol is

esterified and lysophospholipids are created from phospholipids by LCAT treatment, the vesicular structure of Lp-X is no longer stable. This same process likely explains our current findings. Because LCAT is primarily produced by the liver and first secreted into the sinusoidal space before entering the plasma compartment, it may be able to prevent, during cholestasis, the formation of Lp-X in the sinusoidal space and or at least remodel it after it is transferred there from the hepatocyte. Lp-X may have still formed in WT mice with normal levels of LCAT, because the endogenous level of LCAT may have been insufficient for handling the increased reflux of biliary lipids due to the ANIT treatment. LCAT activity is also known to sharply drop due to any type of liver damage,[47] which could also be another explanation for why WT mice still produced some Lp-X.

In FLD, Lp-X has clearly been shown to cause proteinuria and renal damage.[18] Furthermore, rhLCAT treatment can prevent Lp-X formation in animal models of FLD and prevent renal damage.[18] Acute kidney injury following a wide variety of liver diseases, including cholestasis, is also known to occur[48,49] and is a common outcome in hepatorenal syndrome.[50] In a dog model of cholestasis, Lp-X was shown to be deposited in the glomeruli and cause renal damage[24,25] but the causal role of Lp-X in renal injury in human liver diseases requires additional studies. Lp-X from cholestasis has been clearly shown to cause severe xanthomas, which can be quite disfiguring, particularly in Allagile syndrome[12] and is due to the uptake of Lp-X by dermal macrophages.[23] The pathogenesis is not well understood, but Lp-X has also been implicated in neuropathy, which can sometimes develop in patients with longstanding cholestasis.[8] Another potential indication for developing a treatment to lower Lp-X in cholestasis is hyperviscosity syndrome.[27] Some cholestatic patients can develop such high levels of Lp-X that it can increase the viscosity of plasma to such a degree that it impedes blood flow and can precipitate life-threating strokes.[27]

Oral lipid-reducing medications, such as statins, and fibrates, have been tried to lower Lp-X in cholestasis, but they are usually ineffective.[51] Besides treating the underlying cause of cholestasis, the only effective treatment to lower Lp-X is plasma exchange.[8] It can acutely lower Lp-X, leading to the normalization of alkaline phosphatase, total bilirubin and AST. Based on the results of this study, rhLCAT, which has been shown to be safe in early stage clinical trials,[21,22] could also be a potential therapy. rhLCAT is delivered by intravenous infusion and has a half-life of several days,[21,22] so it would be difficult to use as a chronic therapy, but it may be useful for the acute management of cholestatic patients. There are also early efforts to develop small molecule activators of LCAT,[52] which could be a future consideration as a therapy for this disorder.

In summary, our results demonstrate that LCAT can reduce the formation of Lp-X in a mouse model of cholestasis, which extends the possible indications for rhLCAT therapy.

## ACKNOWLEDGEMENT

This work was supported by the intramural funds from the National Heart, Lung, and Blood Institute at the National Institutes of Health and a CRADA research grant from MedImmune Inc.

## DISCLOSURE

The authors declare that the research was conducted in the absence of any commercial or financial relationships that could be construed as a potential conflict of interest.

## AUTHOR CONTRIBUTIONS

Amar, Karathanasis, and Remaley participated in research design. Amar, Freeman, Neufeld, Nishida, and Pryor conducted experiments. Amar, Freeman, Neufeld, Sampson, and Nishida performed data analysis. Amar, Neufeld, Freeman, Karathanasis, and Remaley wrote or contributed to the writing of the manuscript.

## PROTECTION OF ANIMALS IN RESEARCH

All animal studies were approved by the NHLBI Animal Care and Use Committee (protocols # H-0050, H-0018). All animal studies followed the institutional and national guide for the care and use of laboratory animals.

## ORCID

*Marcelo J. A. Amar* https://orcid.org/0000-0002-9097-2422

## REFERENCES

1. Seidel D, Alaupovic P, Furman RH, McConathy WJ. A lipoprotein characterizing obstructive jaundice. II. Isolation and partial characterization of the protein moieties of low density lipoproteins. *J Clin Invest*. 1970;49:2396-2407.
2. Narayanan S, Seidel D. Lipoprotein-X. *CRC Crit Rev Clin Lab Sci*. 1979;11:31-51.
3. Komoda T *The HDL Handbook: Biological Functions and Clinical Implications*. Second edn. Amsterdam; Boston: Elsevier/AP, Academic Press is an imprint of Elsevier; 2014.
4. Ritland S, Sauar J, Holme R, Blomhoff JP. The electrophoretic mobility of lipoprotein X in postheparin plasma. *Clin Chim Acta*. 1977;75:129-135.
5. Freeman LA, Shamburek RD, Sampson ML, et al. Plasma lipoprotein-X quantification on filipin-stained gels: monitoring recombinant LCAT treatment ex-vivo. *J Lipid Res*. 2019;60:1050–1057.
6. Hohenester S, Oude-Elferink RP, Beuers U. Primary biliary cirrhosis. *Semin Immunopathol*. 2009;31:283-307.
7. Kaplan MM, Gershwin ME. Primary biliary cirrhosis. *N Engl J Med*. 2005;353:1261-1273.
8. Brandt EJ, Regnier SM, Leung EKY, et al. Management of lipoprotein X and its complications in a patient with primary sclerosing cholangitis. *Clin Lipidol*. 2015;10:305-312.
9. Johnson P. Studies in cholestasis of pregnancy with special reference to lipids and lipoproteins. *Acta Obstet Gynecol Scand Suppl*. 1973;27:1-80.
10. Weidman SW, Ragland JB, Sabesin SM. Plasma lipoprotein composition in alcoholic hepatitis: accumulation of apolipoprotein E-rich high density lipoprotein and preferential reappearance of "light'-HDL during partial recovery. *J Lipid Res*. 1982;23:556-569.
11. Duchnowska A, Wach K, Poradowska W. Lipoprotein X (LP-X) in the differential diagnosis of cholestasis in children, with special reference to biliary atresia. *Probl Med Wieku Rozwoj*. 1979;8:84-91.
12. Davit-Spraul A, Pourci ML, Atger V, et al. Abnormal lipoprotein pattern in patients with Alagille syndrome depends on Icterus severity. *Gastroenterology*. 1996;111:1023-1032.
13. Turchin A, Wiebe DA, Seely EW, Graham T, Longo W, Soiffer R. Severe hypercholesterolemia mediated by lipoprotein X in patients with chronic graft-versus-host disease of the liver. *Bone Marrow Transplant*. 2005;35:85-89.

14. Remaley AT. Commentary. *Clin Chem*. 2015;61:1032.
15. Manzato E, Fellin R, Baggio G, Walch S, Neubeck W, Seidel D. Formation of lipoprotein-X. Its relationship to bile compounds. *J Clin Invest*. 1976;57:1248-1260.
16. Rousset X, Vaisman B, Amar M, Sethi AA, Remaley AT. Lecithin: cholesterol acyltransferase–from biochemistry to role in cardiovascular disease. *Curr Opin Endocrinol Diabetes Obes*. 2009;16:163-171.
17. Lynn EG, Choy PC, Magil A, Karmin O. Uptake and metabolism of lipoprotein-X in mesangial cells. *Mol Cell Biochem*. 1997;175:187-194.
18. Ossoli A, Neufeld EB, Thacker SG, et al. Lipoprotein X causes renal disease in LCAT deficiency. *PLoS ONE*. 2016;11:e0150083.
19. Vaisman BL, Neufeld EB, Freeman LA, et al. LCAT enzyme replacement Therapy reduces LpX and improves kidney function in a mouse model of familial LCAT deficiency. *J Pharmacol Exp Ther*. 2019;368:423–434.
20. Rousset X, Vaisman B, Auerbach B, et al. Effect of recombinant human lecithin cholesterol acyltransferase infusion on lipoprotein metabolism in mice. *J Pharmacol Exp Ther*. 2010;335:140-148.
21. Shamburek RD, Bakker-Arkema R, Auerbach BJ, et al. Familial lecithin:cholesterol acyltransferase deficiency: first-in-human treatment with enzyme replacement. *J Clin Lipidol*. 2016;10:356-367.
22. Shamburek RD, Bakker-Arkema R, Shamburek AM, et al. Safety and tolerability of ACP-501, a recombinant human lecithin: cholesterol acyltransferase, in a phase 1 single-dose escalation study. *Circ Res*. 2016;118:73-82.
23. Suzuki L, Hirayama S, Fukui M, et al. Lipoprotein-X in cholestatic patients causes xanthomas and promotes foam cell formation in human macrophages. *J Clin Lipidol*. 2017;11:110-118.
24. Ritland S, Bergan A. Plasma concentration of lipoprotein-X (LP-X) in experimental bile duct obstruction. *Scand J Gastroenterol*. 1975;10:17-24.
25. Blomhoff JP, Hovig T, Stokke KT, et al. Lipid deposition in kidneys in experimental liver disease: a study in dogs with choledochocaval anastomosis. *Eur J Clin Invest*. 1979;9:267-280.
26. Turchin A, Seifter JL, Seely EW. Clinical problem-solving. Mind the gap. *N Engl J Med*. 2003;349:1465-1469.
27. Rosenson RS, Baker AL, Chow MJ, Hay RV. Hyperviscosity syndrome in a hypercholesterolemic patient with primary biliary cirrhosis. *Gastroenterology*. 1990;98(5 Pt 1):1351-1357.
28. Chisholm JW, Dolphin PJ. Abnormal lipoproteins in the ANIT-treated rat: a transient and reversible animal model of intrahepatic cholestasis. *J Lipid Res*. 1996;37:1086-1098.
29. Vaisman BL, Klein H-G, Rouis M, et al. Overexpression of human lecithin cholesterol acyltransferase leads to hyperalphalipoproteinemia in transgenic mice. *J Biol Chem*. 1995;270:12269-12275.
30. Lambert G, Sakai N, Vaisman BL, et al. Analysis of glomerulosclerosis and atherosclerosis in lecithin cholesterol acyltransferase-deficient mice. *J Biol Chem*. 2001;276:15090-15098.
31. Sakurai T, Sakurai A, Vaisman BL, et al. Development of a novel fluorescent activity assay for lecithin:cholesterol acyltransferase. *Ann Clin Biochem*. 2018;55:414-421.
32. Vaisman BL, Demosky SJ, Stonik JA, et al. Endothelial expression of human ABCA1 in mice increases plasma HDL cholesterol and reduces diet-induced atherosclerosis. *J Lipid Res*. 2012;53:158-167.
33. Tanaka Y, Aleksunes LM, Cui YJ, Klaassen CD. ANIT-induced intrahepatic cholestasis alters hepatobiliary transporter expression via Nrf2-dependent and independent signaling. *Toxicol Sci*. 2009;108:247-257.
34. Thacker SG, Rousset X, Esmail S, et al. Increased plasma cholesterol esterification by LCAT reduces diet-induced atherosclerosis in SR-BI knockout mice. *J Lipid Res*. 2015;56:1282-1295.
35. Felker TE, Hamilton RL, Havel RJ. Secretion of lipoprotein-X by perfused livers of rats with cholestasis. *Proc Natl Acad Sci USA*. 1978;75:3459-3463.
36. Fellin R, Manzato E. Lipoprotein-X fifty years after its original discovery. *Nutr Metab Cardiovasc Dis*. 2019;29:4-8.
37. Cullen JM, Faiola B, Melich DH, et al. Acute alpha-naphthylisothiocyanate-induced liver toxicity in germfree and conventional male rats. *Toxicol Pathol*. 2016;44:987-997.
38. Chatterjee S, Annaert P. Drug-induced cholestasis: mechanisms, models, and markers. *Curr Drug Metab*. 2018;19:808-818.
39. Goldfarb S, Singer EJ, Popper H. Experimental cholangitis due to alpha-naphthyl-isothiocyanate (ANIT). *Am J Pathol*. 1962;40:685-698.
40. Elferink RP, Ottenhoff R, van Marle J, Frijters CM, Smith AJ, Groen AK. Class III P-glycoproteins mediate the formation of lipoprotein X in the mouse. *J Clin Invest*. 1998;102:1749-1757.
41. Crawford AR, Smith AJ, Hatch VC, Oude Elferink RP, Borst P, Crawford JM. Hepatic secretion of phospholipid vesicles in the mouse critically depends on mdr2 or MDR3 P-glycoprotein expression. Visualization by electron microscopy. *J Clin Invest*. 1997;100:2562-2567.
42. Homolya L, Fu D, Sengupta P, et al. LKB1/AMPK and PKA control ABCB11 trafficking and polarization in hepatocytes. *PLoS ONE*. 2014;9:e91921.
43. Claudia Fuchs VM, Tardelli M, Remetic J,, et al. Absence of BSEP (ABCB11) protects MDR2 (ABCB4) KO mice from cholestatic liver and bile duct injury through anti-inflammatory bile acid composition and signaling. *J Hepatol*. 2019;70:E163-E164.
44. Da Silva K. HDL beyond cholesterol. *Nat Med*. 2014;20:250.
45. Barter PJ, Nicholls S, Rye KA, Anantharamaiah GM, Navab M, Fogelman AM. Antiinflammatory properties of HDL. *Circ Res*. 2004;95:764-772.
46. Karathanasis SK, Freeman LA, Gordon SM, Remaley AT. The changing face of HDL and the best way to measure it. *Clin Chem*. 2017;63:196-210.
47. Tahara D, Nakanishi T, Akazawa S, et al. Lecithin-cholesterol acyltransferase and lipid transfer protein activities in liver disease. *Metabolism*. 1993;42:19-23.
48. Deep A, Saxena R, Jose B. Acute kidney injury in children with chronic liver disease. *Pediatr Nephrol*. 2019;34:45-59.
49. Aniort J, Poyet A, Kemeny JL, Philipponnet C, Heng AE. Bile cast nephropathy caused by obstructive cholestasis. *Am J Kidney Dis*. 2017;69:143-146.
50. Amin AA, Alabsawy EI, Jalan R, Davenport A. Epidemiology, pathophysiology, and management of hepatorenal syndrome. *Semin Nephrol*. 2019;39:17-30.
51. Sorokin A, Brown JL, Thompson PD. Primary biliary cirrhosis, hyperlipidemia, and atherosclerotic risk: a systematic review. *Atherosclerosis*. 2007;194:293-299.
52. Freeman LA, Demosky SJ, Konaklieva M, et al. Lecithin: cholesterol acyltransferase activation by sulfhydryl-reactive small molecules: role of cysteine-31. *J Pharmacol Exp Ther*. 2017;362:306-318.

## SUPPORTING INFORMATION

Additional supporting information may be found online in the Supporting Information section.

**How to cite this article:** Amar MJA, Freeman LA, Nishida T, et al. LCAT protects against Lipoprotein-X formation in a murine model of drug-induced intrahepatic cholestasis. *Pharmacol Res Perspect*. 2019;00:e00554. https://doi.org/10.1002/prp2.554